2nd Symposium on The Lift and Escalator Technologies

Analysis of the frequency behaviour for vertical motions in elevator systems

Ingo Pletschen[1], Stephan Rohr[1] and Ralph Kennel[2]

[1] ThyssenKrupp Aufzugswerke, Bernhäuserstr. 45, 73765 Neuhausen a.d.F., Germany,
Email: ingo.pletschen@thyssenkrupp.com,

[2] Technische Universität München, Arcisstr. 21, 80333 Munich, Germany,
Email: eal@ei.tum.de

INTRODUCTION

Knowledge about the transfer function and the frequency behaviour for elevator systems is of interest for several aspects. For example, to analyse the sensitivity of the cabin to specific frequencies, which may causes mechanical and acoustical vibrations and thus results in discomfort. In addition the frequency behaviour is of high interest while applying control algorithms for active vibration suppression or cabin position control [1]. Due to the different suspension rope length, depending on the cabin's position, the transfer function is time-varying during the travel on one hand. On the other hand it depends on the cabin's payload. Existing literature concentrates on the frequency response analysis lower than 20 Hz [2], while this paper concentrates on methods and measurement signals which are precise enough to determine the frequency behaviour up to 100 Hz. In addition a wide range of elevator constructions exists, which differs for example in roping, number of rope pulleys or the location of isolation elements. For the model validation of numerous elevator constructions a method is needed, which may be easily applied to many elevators and preferably does not need additional measurement sensors.

At first, this paper describes different measurement possibilities and input shapes for the identification process. It is analysed which input and output signal produce meaningful transfer functions and how they can be compared to each other. Afterwards the different identification methods are described, which is followed by the description how the experiments have been conducted at a real elevator. Finally, the frequency behaviours are discussed, which are obtained at a low-rise elevator for different cabin positions and payloads.

METHODS FOR SPECTRAL ANALYSIS IN ELEVATORS

Determining the frequency behaviour it is of specific interest to know the resonance frequencies of the system. While the resonance frequencies apply for the whole system, the peaks of the transfer function depend on the chosen input and output signals. Thus meaningful signals have to be chosen to ensure that all system resonances are represented in the transfer function. It is advantageous to use excitation and measurement signals which are already available in the system and thus determining the frequency behaviour may be conducted in many elevators, easily. This is especially important, as elevators are constructed in many different ways concerning the roping, rope pulleys and the position of spring elements, which results in different frequency behaviour.

In state of the art elevators, often permanent magnet machines with a frequency converter and a position encoder with sine/cosine traces are used. Thus, the currents, voltages and traction sheave position/velocity are available in a high precision and in a high frequency. In this paper the set current i^*_q is used for excitation, while actual current $i_{q,act}$ and actual rotational velocity ω_{act} are evaluated to determine the frequency behaviour of the elevator. This dependence is shown in the block diagram of figure 1 and for the modelling of the mechanical system the reader may refer to

[1]. If other measurement signals are used, e.g. cabin or counterweight acceleration [2], additional sensors are needed as they are usually not installed in elevators. The data of different sensors also have to be accurately synchronized as otherwise the calculation yields a wrong transfer function. This is with less effort ensured for the current and traction sheave velocity measurements, as both are captured by the frequency converter.

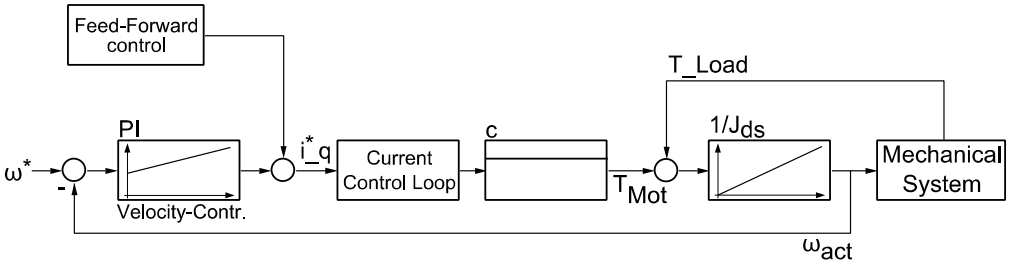

Figure 1: Overview cascaded control structure

Several Methods for the identification of the transfer functions in the frequency or time domain exits [3]. In the following the frequency response analysis (FRA) with a pseudo random binary signal (PRBS) as excitation is described. In addition the excitation with a single discrete frequency and the evaluation with the orthogonal correlation method are considered.

Transfer functions in elevators

In literature transfer functions with different input and output signals are analysed which makes it difficult to compare the results. In addition, if less meaningful input and output signals are chosen, the peaks in the transfer function do not represent the system resonances. In [1] the transfer function $G_{aC,Tmot}$ from motor torque T_{mot} to car acceleration a_C is used, which is, except for a constant factor, the same like $G_{FC,Fmot}$ from motor force F_{mot} to car force F_C [4]. In the following and in [5] the frequency behaviour $G_{\omega,Tmot}$ from motor torque T_{mot} to traction sheave angular velocity ω_{act} is regarded. Furthermore, in [2] the transfer function $G_{vC,vT}$ from traction sheave velocity v_T to car velocity v_C is used.

In this section the similarities and differences of the transfer function are showed up, while analysing the poles and zeros of a simplified 3-mass model. The equations are described in [1][4] and yield the following differential equations which are solved via the Laplace operator

$$F_C = m_C a_C = (v_T - v_C)D_C + (x_T - x_C)C_C \tag{1}$$

$$\rightarrow F_C = \frac{m_C(d_C s^2 + c_C s)}{(s^2 + d_C s + c_C)}(v_T) \tag{2}$$

$$\rightarrow F_{CW} = \frac{m_{CW}(d_{CW} s^2 + c_{CW} s)}{(s^2 + d_{CW} s + c_{CW})}(-v_T) \tag{3}$$

Here $d_C = D_C/m_C$, $C_C = C_C/m_C$, describes damping and spring constant of the rope on the cabin's side. Indices $_{CW}$ represent the variable on the counterweight side. Furthermore x_T and x_C are the displacements of traction sheave and cabin.

Via the relation $F_C = m_C \cdot v_C \cdot s$, equation (2) yields the transfer function listed in equation (4) from traction sheave velocity v_T to car velocity v_C.

$$G_{vC,vT}(s) = \frac{v_C}{v_T} = \frac{(d_C s + c_C)}{(s^2 + d_C s + c_C)} \tag{4}$$

This represents the differential equation with forced velocity excitation at the traction sheave. Then the parameters of the counterweight's side have no impact on the resonance frequencies. The behaviour is equivalent when the brake is closed and the cabin is excited. With the forced velocity excitation and elevators with compensation ropes the counterweight parameters influence the transfer function only via the compensation sheave, however not via the traction sheave.
Equation (5) results from equation (3), if the traction sheave is excited via the motor torque. Via transposition of equation (5) this yields the function $G_{\omega,Tmot}$, which is displayed in equation (6).
Here the static forces due to gravity are neglected and only the d'Alembert forces which influence the frequency behaviour are considered.

$$\omega_{act} = \frac{1}{sJ_T}\left(T_{mot} - \frac{m_{CW}(d_{CW}s^2+c_{CW}s)}{(s^2+d_{CW}s+c_{CW})}\omega_{act}r_T^2 - \frac{m_C(d_Cs^2+c_Cs)}{(s^2+d_Cs+c_C)}\omega_{act}r_T^2\right) \quad (5)$$

$$G_{\omega,Tmot}(s) = \frac{\omega_{act}}{T_{mot}} = \frac{v_T}{r_T T_{mot}} = \frac{1}{sJ_T}\left(\frac{(s^2+d_{CW}s+c_{CW})(s^2+d_Cs+c_C)}{(s^2+d_{CW}s+c_{CW})(s^2+d_Cs+c_C)+m_{CW}r_T^2(d_{CW}s^2+c_{CW}s)(s^2+d_Cs+c_C)+m_Cr_T^2(d_Cs^2+c_Cs)(s^2+d_{CW}s+c_{CW})}\right) \quad (6)$$

Out of this also the transfer function between motor force F_{mot} to car force F_C is derived in the following equations.

$$G_{\omega,T}(s) = \frac{v_T}{r_T T_{mot}} \quad (7)$$

$$\rightarrow G_{\omega,T}(s)\frac{v_C}{v_T} = \frac{v_T}{r_T T_{mot}}\frac{v_C}{v_T} = \frac{v_T}{r_T^2 F_{mot}}\frac{F_C}{s\, m_C v_T} \text{ with } v_C = \frac{F_C}{s\, m_C} \quad (8)$$

$$\rightarrow G_{Fc,Fmot}(s) = \frac{F_C}{F_{mot}} = G_{\omega,Tmot}(s)\cdot G_{vC,vT}(s)\cdot s\, m_C r_T^2 \quad (9)$$

As visible from above equations the transfer functions $G_{FC,Fmot}$ and $G_{\omega,Tmot}$ are dependent also on the suspended masses and the elasticity of the suspension ropes at the counterweight side. Looking at $G_{FC,Fmot}$ (eq. (9)) it results, that the poles from $G_{vC,vT}$ (eq. (4)) are cancelled via the zeros of $G_{\omega,Tmot}$. Thus $G_{FC,Fmot}$ has the same denominator and poles like $G_{\omega,Tmot}$, however slightly different zeros. Therefore the resonance frequencies are the same, while antiresonance frequencies differs. In comparison $G_{vC,vT}$ has different poles and respectively resonances. With the forced velocity excitation the counterweight's influence over the traction sheave to the cabin is not considered. Thus the function $G_{vC,vT}$ is only meaningful for a part of the elevator system.

Frequency Response Analysis

Most identification schemes are only valid for transfer functions which are time-invariant during the identification process [4]. This requires in elevators that the cabin stays at the same position, as otherwise the transfer function changes [1]. Thus identification cannot be performed during higher speeds and only small motions around a constant cabin position are allowed. Therefore the static and coulomb friction influences the transfer function [1].
For the frequency response analysis the elevator system is excited by the torque generating set current i^*_q with a pseudo random binary signal (PRBS), which beginning is shown in figure 2. In this paper the sample time T_s has been chosen to 1.008 ms, which results with the Shannon theorem in a frequency range up to 496 Hz. Additionally a 13bit PRBS is used, which results with equation (10) in a measurement time for each sequence of 8.26 s. During this time the PRBS is uncorrelated, which is a mandatory requirement for the frequency response analysis [3]. Afterwards the PRBS is reiterated several times, to obtain a less noisy result. This has a frequency resolution of the transfer function of 0.12 Hz as displayed in equation (11).

$$T_M = (2^{13}\text{-}1)\cdot 1.008e^{-3}\text{ s} = 8.26\text{ s} \quad (10)$$

$$f_{res} = 1/ T_s = 0.12 \text{ Hz} \quad (11)$$

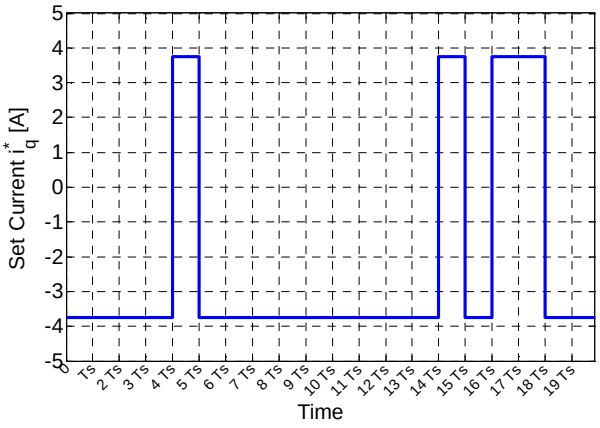

Figure 2: Pseudo Random Binary Signal

The spectral densities $S_{uy}(f)$, $S_{uu}(f)$ are determined while calculating the cross/auto spectral density between input signal *u* and output signal *y*. Then the transfer function is given by equation (12).

$$G(f) = S_{uy}(f) / S_{uu}(f) \quad (12)$$

For determination of the open loop transfer function from actual motor torque T_{mot} to actual speed ω_{act} the velocity controller is set to a low bandwidth to avoid influence from the feedback. In equation (12) the input signal *u* is represented by the actual current $i_{q,act}$, while the output *y* is ω_{act}. With this procedure the non-parametric transfer function $G(s)=\omega_{act}(s)/T_{mot}(s)$ is obtained, where motor torque is given for permanent magnet machines by $T_{mot} = c \cdot i\_q_{act}$. The transfer function in equation (12) has complex numbers, thus a common way to illustrate the frequency behaviour is via bode plots, which display the absolute value and phase.

For evaluation of the calculated transfer functions the coherence is chosen as assessment criterion and given in equation (13).

$$\gamma^2 = |S_{uy}(f)|^2 / (S_{uu}(f) \cdot S_{yy}(f)) \quad (13)$$

If the system has strongly linear dependence, then the coherence equals one. Otherwise it is less than one, which occurs also at the location of resonance frequencies [4].

Orthogonal Correlation Method

The orthogonal correlation procedure may be used to determine the frequency behaviour and excites the system with single frequencies via a sine function [3][6]. In figure 3 the scheme of the method is displayed with the amplitude of the set current $\hat{u}$ which excites the single frequency f_0. The system is excited using a sine signal during the measurement time *Tm*. With this estimation method the real and imaginary parts are obtained for the transfer functions

$$G_1(s) = \omega_{act}(s) / i^*_q(s) \quad (14)$$
$$G_2(s) = i_{q,act}(s)/ i^*_q(s) \text{ with } s=j2\pi f_0 . \quad (15)$$

Out of these the complex transfer function between actual current to actual speed is given by $G(s)= G_1(s)/ G_2(s)$ and the gain $|G|$ may be calculated via $|G_1(s)/ G_2(s)|$. This is reiterated for several discrete frequencies and the data is added to the resulting bode plots of previous section. Also here, the velocity controller is set to a low bandwidth as described in the previous section.

Advantageous of the orthogonal correlation method is the concentration of the total energy of the excitation signal to one frequency. This yields more accurate results, especially if non-linearities like friction or quantization inaccuracies are present. In contrast the energy of the PRBS is distributed over the whole frequency range and thus each single frequency is less excited.

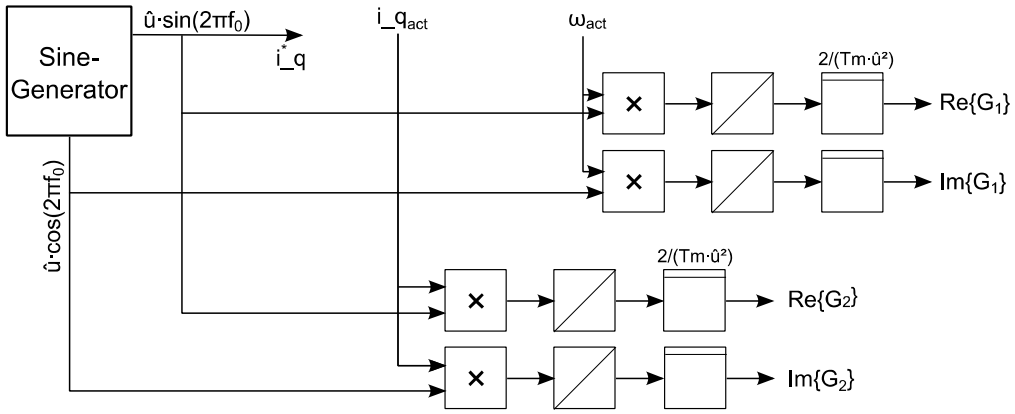

Figure 3: Scheme of orthogonal correlation

EXPERIMENTAL SETUP

To apply the tests to many elevator constructions, the experimental setup should be easily installed. In figure 4 the general setup is shown, where the elevator controller is unplugged and instead a dSPACE box is plugged to the CAN-buses. The box controls the frequency converter via the first CAN-bus for slow signals - e.g. initiating, open brakes, cabin position, load sensor signal or set speed. It also provides via the second CAN-bus the fast signals, like the set current excitation and also the captured sensor data from the frequency converter is exchanged. The captured data is offline processed and then the transfer function is calculated.

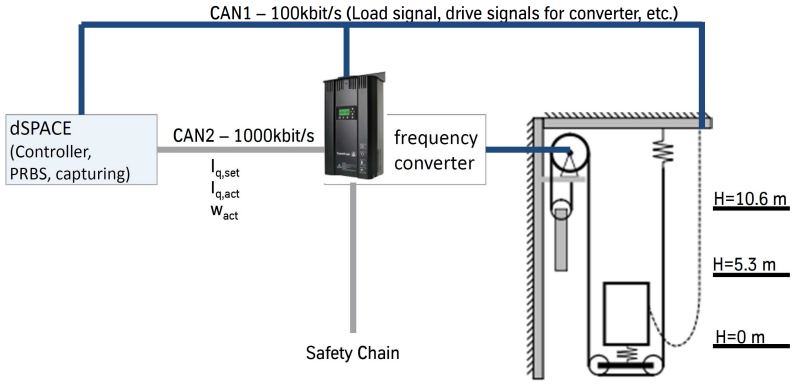

Figure 4: Experimental setup

The basic safety is ensured via the safety chain, which is coupled to the frequency converter. It would stop the drive, if e.g. the elevator would move to the end switches of the shaft.

The test elevator used in this paper has a travel height of 10.6 m, a 2:1 roping and a maximum payload of 450 kg. Further parameters are listed in table A.1.

EXPERIMENTAL RESULTS

The experiments have been performed for different cabin positions and loads. In figure 5 the results are shown for different cabin positions, while the payload is held constant at m_L=180 kg. The distance in meters has its origin in the bottom floor, referring to H=0 m. Therefore, the distance 9.6 m is shortly below the top floor, which is located at H=10.6 m. The first resonance frequency at 5 Hz stays constant for this elevator. The second resonance is also distinctive and increases with lower cabin position. The reason is found in the short suspension ropes between counterweight and traction sheave when the cabin is in bottom position. This results in a very stiff coupling between counterweight and traction sheave. This coupling is stiffer than the coupling when the cabin is in top position as the cabin is additionally isolated via the cabin springs. This behaviour is also confirmed by the theory of a simplified three mass model, while looking at the poles of the transfer function (eq. 6). If typical parameters are inserted it results in a higher second resonance frequency when the cabin is in bottom position and the counterweight is not isolated with additional springs applying to this test elevator.

Further resonances occur above 30 Hz and vary strongly with the cabin's position. Mainly the anti-resonances or the zeros of the transfer function change the location, which thus may eliminate or reduce the peak of a resonance. Especially, this is visible for the cabin in top position and the first resonance.

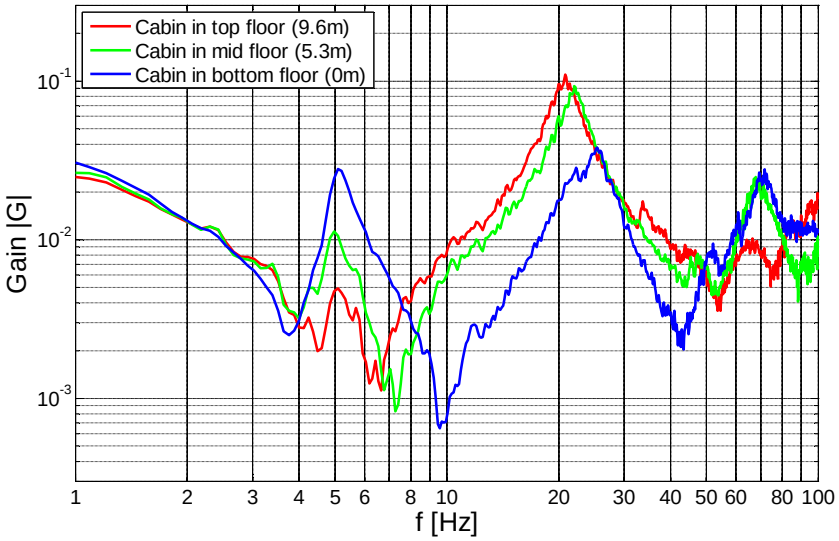

Figure 5: Bode plot for different positions: $|G(s)| = |\ \omega_{act}(s)/T_{mot}(s)|$; $s=j2\pi f$

Looking at the frequency range up to 10 Hz the transfer function of the elevator with cabin in top position is much noisier than in bottom position. Here, the reason is a higher friction of the cabin in top position, which is also visible in the coherence shown in figure 6 (b). It drops significantly in this range, indicating the non-linear relationship. The strongest friction is caused between guide rails and cabin as well as between the guide rails and counterweight. For this low-rise elevator this influence is stronger as guide shoes are used and would be smaller, if roller guides are installed. Additionally, friction occurs at the traction sheave shaft and also for the rope pulleys at the counterweight and cabin.

The main reasons for the influence of the friction are the identification schemes, which are valid for transfer functions which are time-invariant during the identification process [3]. Time-invariance in the elevator system requires that the cabin stays at the same position, as otherwise the rope length changes and thus the transfer function (see figure 5). Therefore the identification cannot perform during higher speeds and only small motions around a constant cabin position are allowed, which

thus causes in static and sliding friction. During the travel, for non-zero speeds, the friction causes a constant force in opposite of the direction of travel, which results only in a different value for the constant frequency content at zero Hertz, however not for the other frequencies. Therefore the static and sliding friction influence the identification process.

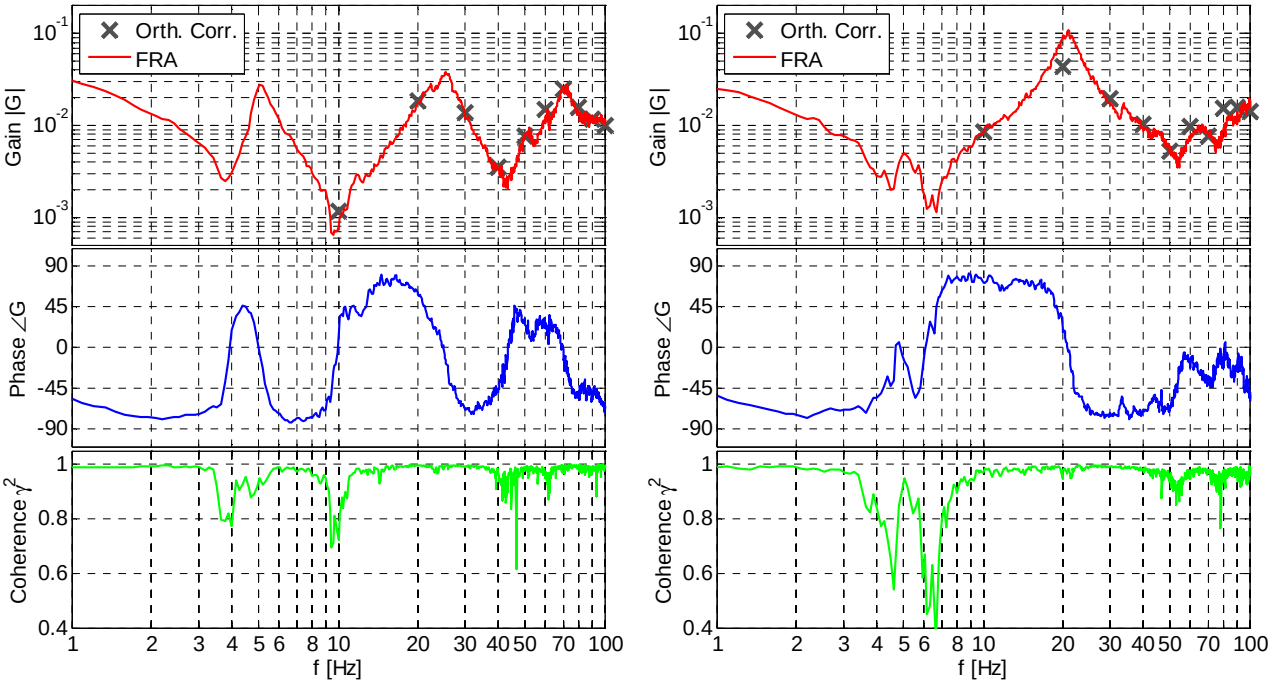

(a) m_L = 180 kg, H = 0 m (b) m_L = 180 kg, H = 9.6 m

Figure 6: Transfer functions $G(s) = \omega_{act}(s)/T_{mot}(s)$; $s=j2\pi f$

In figure 6 and figure 7 (a) also the results of the orthogonal correlation are marked with the grey crosses. In general the crosses fit very well on the transfer function estimated by the FRA. Small differences occur in figure 6 (b) at 20Hz, where the peak is directly located at a resonance and is the reason for the deviation. As expected, it is also visible, that the small deviations occur when the coherence drops.

While looking at the phase, it shows the same relationships like the gain and the effect of resonances is apparent. Especially, this is visible in figure 7 (b), when the payload is removed and thus the first antiresonance occurs at a higher frequency. This results almost in an elimination of the first resonance, which is visible at the gain. However, the phase indicates even more clearly this elimination and only a small rise and drop in phase occurs between 4 and 5 Hz.

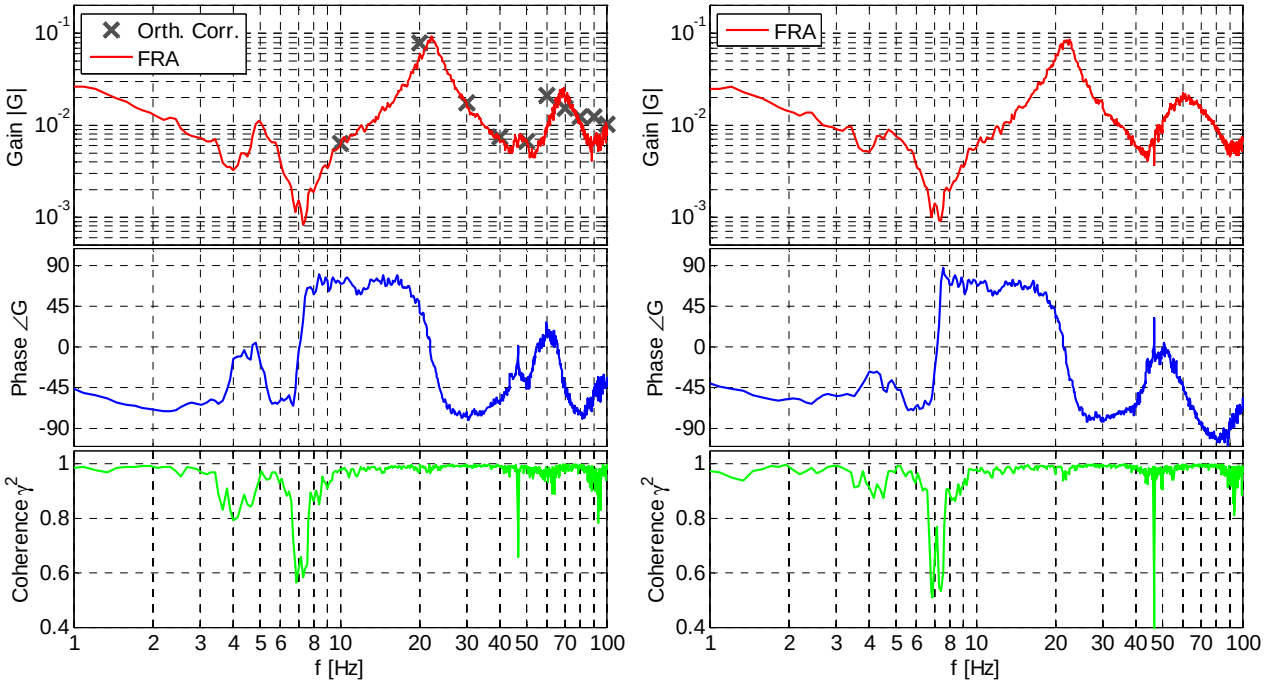

(a) m_L = 180 kg, X_K = 5.3 m (b) m_L = 0 kg, X_K = 5.3 m

Figure 7: Transfer functions $G(s) = \omega_{act}(s)/T_{mot}(s)$; $s=j2\pi f$

SUMMARY

This paper describes two methods to obtain the frequency behaviour for the vertical motion of elevators. The sensor signals are chosen by means of availability in standard elevators and yield accurate results up to 100 Hz. The methods are applied at a test elevator and the frequency behaviour is obtained for several cabin positions and payloads. Both methods give meaningful and also very similar results.

Now, the results can be used to reduce vibrations while optimizing mechanical parameters like spring stiffness or rope pulley inertia. The results may be also used to validate simulation models and thus enable the optimization of elevators already in simulation.

REFERENCES

[1] J.K. Kang, and S.K. Sul: *Vertical-vibration control of elevator using estimated car acceleration feedback compensation*, IEEE Transactions on Industrial Electronics, 47, pp. 91-99, (2000).

[2] Y.M. Cho, and R. Rajamani, *Identification and experimental validation of a scalable elevator vertical dynamic model*, Control Engineering Practice, 9, pp. 181–187, (2001).

[3] R. Isermann: *Identifikation dynamischer Systeme* 1, Springer, (1992).

[4] Claudia Schmidt-Milkau: *Ein Beitrag zur adaptiven Lageregelung von Getriebe-aufzugsanlagen mittlerer Leistung*, PhdThesis, TU Berlin, (1988).

[5] I. Pletschen, S. Rohr, and R. Kennel: *Comparison of simulation models for elevator systems*, Elevator Technology 19, (2012).

[6] I. Pletschen, S. Rohr, and R. Kennel: *Inertia estimation of servo drives with elastically attached masses*. IET Power Electronics, Machines & Drives conference, (2012).

APPENDIX

m_c [kg]	585	Cabin mass
m_L [kg]	450	Maximum payload
m_{cw} [kg]	765	Counterweight mass
H [m]	10.6	Travel height
J_{ds} [kg m²]	0.18	Motor + traction sheave inertia
r_{ds} [m]	0.22	Radius traction sheave
c [Nm/A]	22.7	Motor constant
U	2:1	Roping
N	6	Number of ropes
D_{rope} [mm]	6	Rope diameter

Table A.1: Parameters of test elevator